EVALUATION OF EROSIVE WEAR RESISTANCE OF TiN COATINGS BY A SLURRY JET IMPACT TEST

EVALUATION OF EROSIVE WEAR RESISTANCE OF TiN COATINGS BY A SLURRY JET IMPACT TEST

Y. Iwai, T. Miyajima, T. Honda, Department of Mechanical Engineering, University of Fukui, Bunkyo 3-9-1, Fukui, 910-8507, Japan, iwai@mech.fukui-u.ac.jp
T. Matsubara, Macoho Co. Ltd., Niigata, Japan
K. Kanda, Nachi-Fujikoshi Co. Ltd., Toyama, Japan
S. Hogmark, Uppsala University, Uppsala, Sweden

ABSTRACT

In this paper, it is proposed to use a new type of solid particle impact test (slurry jet) to swiftly evaluate wear properties of thin, single layered or multilayered coatings. By the slurry jet, 1.2 μm alumina particles were impacted at high velocity perpendicular to thin PVD coatings of TiN deposited on high speed steel substrate materials under various substrate temperatures.

Since the coatings have a much higher wear resistance than the substrate material, the wear rate increases significantly to the higher level of the HSS material when the coatings are penetrated. This is utilized in the quantification of the assessment of coating wear. A ranking of wear resistance and correlations to the coating surface hardness measured by nano-indentation tests, and coating morphology and structures are given and discussed.

It is concluded that the slurry jet test is fast, easy to accomplish, and generates reproducible results. It is also very sensitive to variations in coating quality. Thus, it can be recommended as a screening test when evaluating coatings and coated materials. For the coatings included in this study, the TiN deposited under the highest substrate temperature proved to have the highest wear resistance although it had a relatively low hardness. The wear rate of the TiN coatings varies with the orientation of grains, that is, the {111} orientation that dominates for the high temperature deposition shows a higher wear resistance than the {100} orientation, which corresponds with the cleavage fracture behavior. The fact that the higher temperature generates more defect free TiN coatings will also contribute to a better erosive wear resistance for these coatings.

1 INTRODUCTION

A continuing development of versatile and reliable techniques for evaluation of coated components is important for the development of new coating composites and their applications. There exist many studies on evaluation techniques for tribological

assessment of thin hard coatings [1-4]. In many situations, the wear of materials coated with thin coatings is due to a combination of the properties of the coating material, substrate material and interface. Thus, a general evaluation should distinguish between the properties of the coating and substrate material.

Hutchings [5] has reviewed the application of solid particle erosion testing to coated samples. Erosion testing has proven to be a suitable tool for studies of crack initiation and propagation in thin hard coatings [6]. However, by conventional particle erosion tests such as centrifugal and slurry erosion tests, the failure of thin hard coatings often occurs unevenly and after a short test duration due to a high ratio of particle diameter to coating thickness [7-9]. Therefore, if particle erosion is to be used to evaluate coating properties, impact of very small particles is needed, to be able to detach the coating in a form of small fragments. They should also be focused to a small area of the target.

With this background, a new type of solid particle impact test, the slurry jet impact test, was proposed. It has previously been used to quickly evaluate the wear properties of physical vapour deposited (PVD) coatings [10], and applied to the evaluation of the wear resistance of commercially coated tools [11]. It was concluded that the slurry jet impact test is considerably useful as a screening test for thin hard coatings.In this study, the possibility of the slurry jet impact test has been used to evaluate TiN coatings deposited under slightly different conditions. A ranking of wear resistance and correlations to the coating surface hardness and surface morphology are given and discussed. From the results, it is concluded that the slurry jet impact test can be used as a screening test when evaluating coated materials.

2 EXPERIMENTAL

2.1 Test apparatus and procedure

Figure 1 shows a schematic view of the test apparatus. The details are described elsewhere [10]. The flowing stream of water containing solid particles sucked from the tank is mixed with compressed air in the nozzle, and eventually a slurry jet is ejected at high velocity. The cross-section of the nozzle is a square 3 x 3 mm^2. The jet velocity is regulated by the pressure of the compressed air, but could, unfortunately, not be measured. For the pressure of 0.5 MPa used in this study, the maximum velocity was estimated to

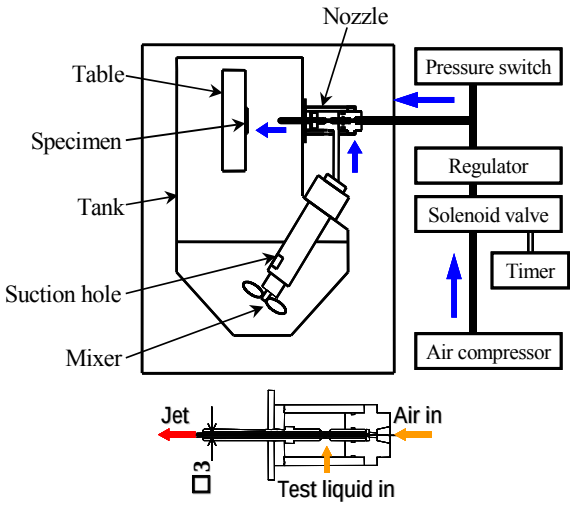

Fig.1 Schematic view of the slurry jet tester. The insert shows detail of the nozzle.

around 100 m/s at the exit of the nozzle. The impingement angle of the jet relative to the test surface was set to α = 90 degrees. The specimen was mounted at 10 mm distance from the end of the nozzle. The test liquid was pure water containing angular alumina particles with an average diameter of 1.2 μm, as erodent. The hardness of the alumina particles ranged from HV= 1800 to 2000 [12]. The concentration of the alumina particles was c= 3 mass % in the tank, and the slurry was kept at room temperature.

The wear loss of the coatings after the tests was too small to be resolved by weighing. Instead, the geometry of the erosion crater was measured with a stylus profilometer at three positions along the centerline of the square wear scar.

2.2 Test materials

Substrate material was high-speed steel (HSS) named SKH57 by Japanese Industrial Standards, with the chemical composition (wt. %) of 1.17-1.15C, 3.0-5.25Mo, 9.0-11.0W, 3.0-3.8V, and 9.0-11.0Co. The hardness of HSS was HV= 950. All substrates were polished to mirror finish. Uncoated HSS was included as a reference material.

TiN was deposited by magnetron sputtering. The substrate voltage was fixed to 100 V. Process gases of Ar and N_2 were supplied at 1.5 and 1.35 m^3/h, respectively, and the pressure of the chamber was about 0.4 Pa.

The coating materials and their properties are listed in Table 1. Three substrate temperatures was used; 330, 390 and 470 ℃, and the corresponding coated specimens are designated TiN-A, B and C, respectively. The TiN coatings had a monolayer structure and their thickness was in the range of 1.8 to 2.1 μm, as estimated from fractured cross-sections. The specimen size was 6 x 6 x 30 mm.

Table 1 Coating materials and their properties

Specimen	Substrate temperature, ℃	Coating thickness, μm
TiN-A	330	2.1
TiN-B	390	1.8
TiN-C	470	1.8

2.3 Measurements of surface properties

The coated surfaces were observed by scanning electron microscopy (SEM) and atomic force microscopy (AFM), and analyzed with X-ray diffraction (XRD). The measurement conditions of the XRD were: copper target, accelerating voltage of 40 kV, beam current of 50 mA and scanning speed of 4°mm^{-1}.

In order to investigate the mechanical properties of the coatings, the nano-scale hardness was measured by a nano-indenter. The indenter was a Berkovich pyramid. Electro-magnetic actuation was used and the displacement was measured by a capacitance gauge. The load was applied in the range of 11.8 to 98.0 mN. Figure 2 shows the penetration depth - load curve. The hardness was calculated by the following equation.

$$H = 3.717 \times 10^{-4} \frac{P_{\max}}{h1^2} \qquad [GPa]$$

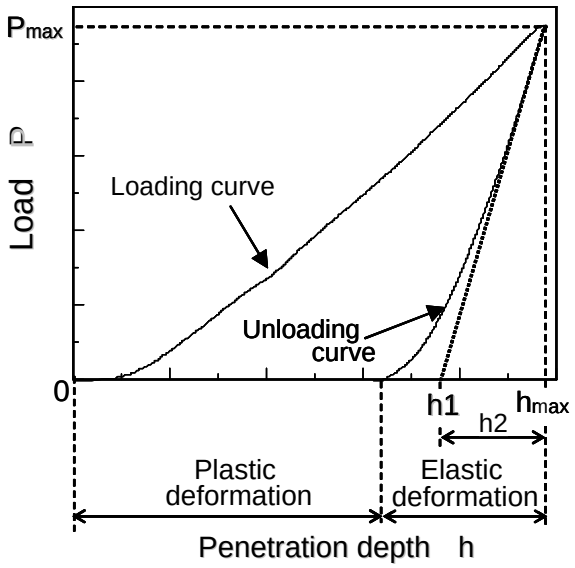

Fig.2 Penetration depth - load curve.

3 RESULTS AND DISCUSSION

3.1 Morphology and hardness of TiN coatings

Figure 3 shows SEM micro-photographs of the original surfaces and fractured cross-sections of the TiN coatings. The grains and pronounced columnar structures can be clearly observed. The grain size increased with increasing substrate temperature. The size of 50 grains was measured at random on the SEM photographs of each specimen. The average size was 0.13, 0.18 and 0.24 μm for the substrate temperatures 330, 390 and 470 ℃, respectively.

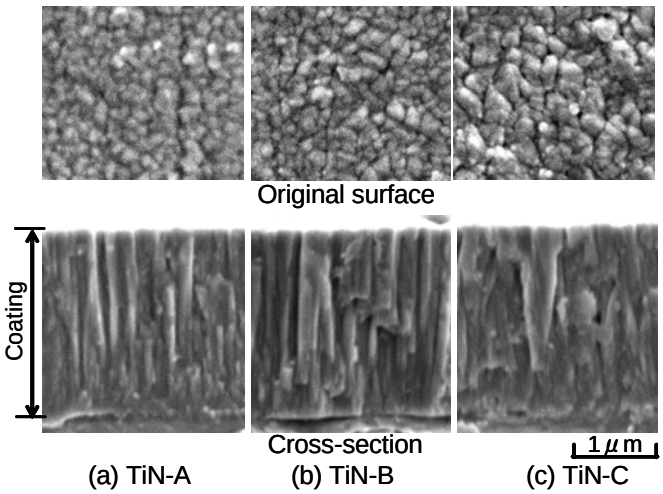

Fig.3 SEM microphotographs of the original surfaces and fractured cross-section of the TiN coatings.

Figure 4 exhibits XRD profiles of the TiN coatings. TiN was found to have a (200) preferred orientation at the substrate temperature of 330 ℃ while it displayed a (111) preferred orientation at 390 and 470 ℃. In addition, the half-value width of the (111) peak narrowed when the substrate temperature increased. Therefore, XRD analysis

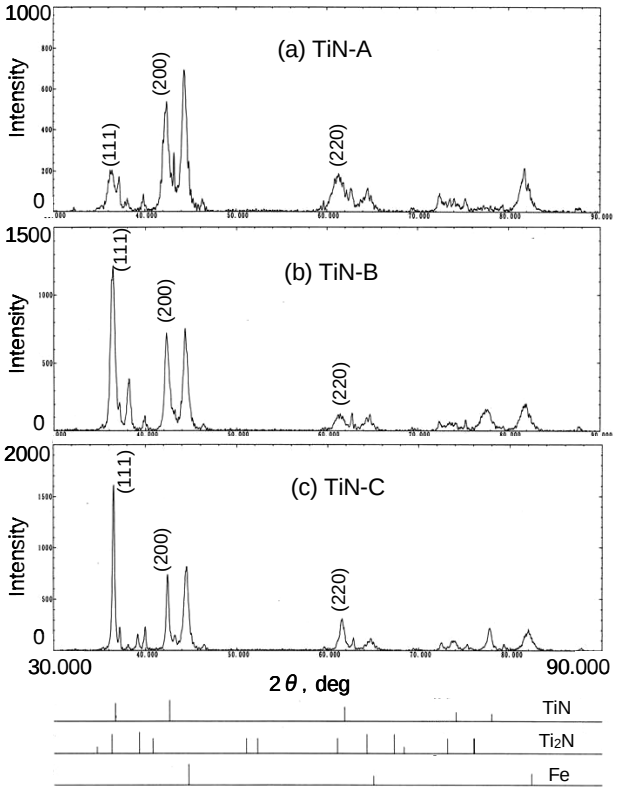

Fig.4 XRD profiles of TiN coated specimens.

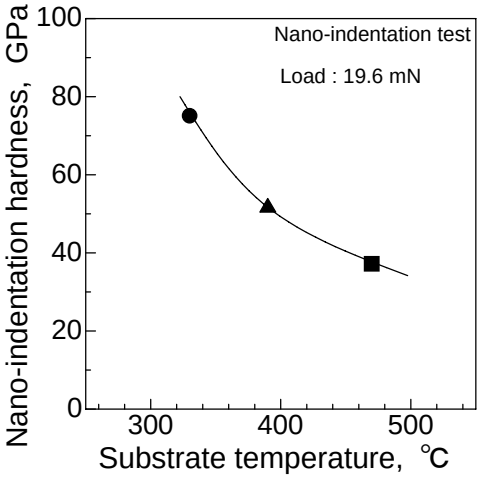

Fig.5 Nano-indentation hardness of TiN coated specimen as a function of substrate temperature.

shows that the grains grow with high preferred orientation and good crystallinity at the highest substrate temperature.

Figure 5 shows the nano-indentation hardness of TiN coated specimen as a function of substrate temperature. A load of 19.6 mN was adopted since it gives a penetration depth smaller than one-fifth to one-tenth of the coating thickness, thus generating values representative of the intrinsic coating properties. The nano-indentation hardness is influenced by the instrument and measuring system, and usually gives relatively high values compared to conventional hardness values of TiN. The nano-indentaion hardness of the TiN coatings decreased with increasing substrate temperature. This result is probably due to the corresponding increase in larger grain with the temperature.

3.2 Wear properties

Figure 6 illustrates the depth profiles of wear craters in the TiN coating, as measured after various test durations. During the first 7.5 min the wear of the coating was gradual and slow, generating a smooth surface, where after the coating was penetrated and severe damage of the substrate commenced. At each test interval the distance between the original and the worn surface at the deepest position was measured and designated as the wear depth.

The wear depth variation with the test duration is shown in Fig.7. For the HSS substrate material, the wear depth increased linearly from the beginning of the test. On the other hand, for TiN coatings, the wear depth increased linearly at a moderate slope until the coating was penetrated after 7.5 to 10 min when it increased significantly. The lines of the coating and of the substrate intersect at a point that completely agrees with the coating thickness. This means that our test is able to determine the wear properties of the thin hard coatings independent of the properties of the substrate. The average slope of the initial part of the wear curve was calculated by means of the least-squares method, and defined to be the coating wear rate.

Figure 8 shows the wear rates of TiN coatings as a function of substrate temperature. In order to confirm the reproducibility of the wear rate of each TiN coating, additional two tests were carried out and their wear rates are also plotted in Fig.8. The standard deviation of the three times tests were 0.0097 to 0.0124 μm/min for each TiN coating. Consequently, our test was found to be highly reproducible. The wear rate decreased with an increase in substrate temperature.

Comparing Fig.8 with Fig.5, the wear rate of TiN deposited at high substrate temperature decreased though its surface hardness became low. This behavior is contrary to the general tendency that abrasive and erosive wear decrease with increasing hardness [12]. Dobrzanski et al. [13] showed that the erosion resistance of TiN deposited on several types of high

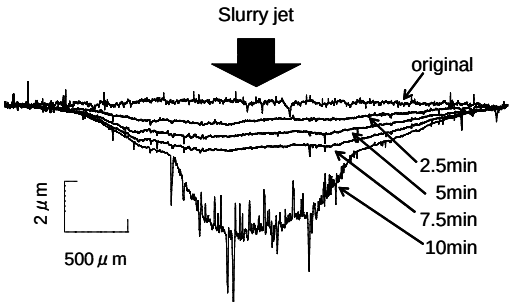

Fig.6 Surface profiles along the center-line of the square erosion scar of TiN-A coating after various test duration.

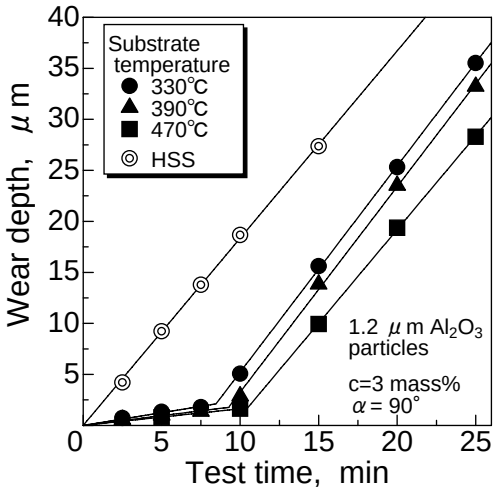

Fig.7 Maximum crater depth of the substrate (HSS) and the TiN coating as a function of test duration.

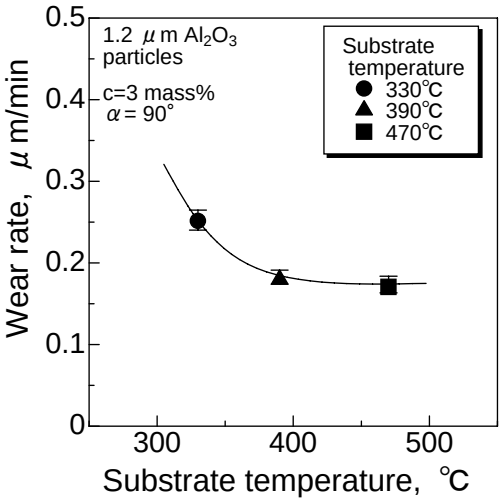

Fig.8 Wear rates of the TiN coatings as a function of substrate temperature.

speed steel increased with the hardness. On the other hand, Soderberg et al. [14] have shown that there is a very minor influence of hardness on resistance to particle erosion within many categories of materials. The explanation is that particle erosion is contradicted by both hardness and ductility. In this case, a higher deposition temperature gives a slightly lower hardness, but also, as evident from the half-width values of the XRD measurements, a more defect free TiN. These two factors point in the direction of increased deformability with deposition temperature. It should be pointed out that the individual erosive impacts in this test occur on such a small scale that there is no influence from the substrate.

3.3 Observation of worn surfaces

Figure 9 shows representative SEM photographs of the worn surface of (c) TiN-A, (d) TiN-C, together with the original surfaces as references. The coatings were worn gradually. For both TiN coatings, a smooth surface was produced and cutting traces and cracks, which usually are characteristic of surfaces exposed to solid particle erosion [12], were neither observed. It is concluded that the material is removed in the form of very small fragments due to attacks from the very small eroding particles.

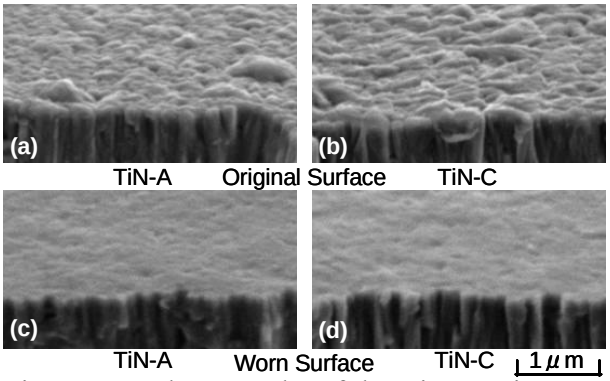

Fig.9 SEM photographs of the TiN coatings.
original surface (a) TiN-A (b) TiN-C
worn surface (c)TiN-A (d) TiN-C

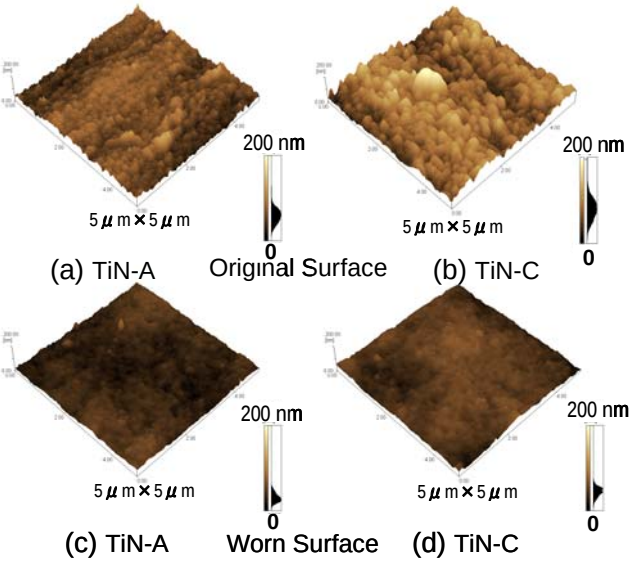

Fig.10 AFM images of the TiN coatings.
original surface (a)TiN-A (b) TiN-C
worn surface (c)TiN-A (d) TiN-C

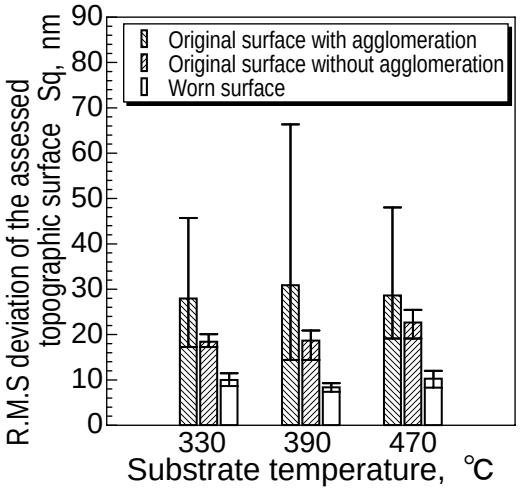

Fig.11 R.M.S. deviation of the assessed topographic surface (Sq) of the original and worn surfaces of the TiN coatings.

The micro topography of the worn surfaces was quantified by AFM, see Fig.10. The original surface of TiN had a regular variation in roughness with agglomeration produced during the coating process. On the other hand, all the worn surfaces of both coatings became very uniform and smooth.

The R.M.S deviation of the assessed topographic surface (Sq) of the original and worn surfaces of the coatings were calculated by 3-D analysis tool [15], see Fig. 11. These results suggest that the size of the detached debris is remarkably smaller than the grain size, which were estimated to several ten nano-meters.

3.4 Relation between surface morphology and wear rate

The ranking of wear resistance of TiN is investigated from the point of view of surface morphology and structure. Figure 12 shows the variation in wear rate of TiN as a function of intensity ratio of (111) to (200) obtained by XRD, see Fig. 4. In the figure, other TiN coatings that were deposited on various HSS or carbon steel at various conditions with different PVD methods are also shown. The wear rates can be plotted on a line and decrease with increasing the ratio regardless of coating conditions. This means that the wear rates of the TiN coatings varies with the orientation of grains, that is, the {111} orientation shows higher wear resistance than the {100}.

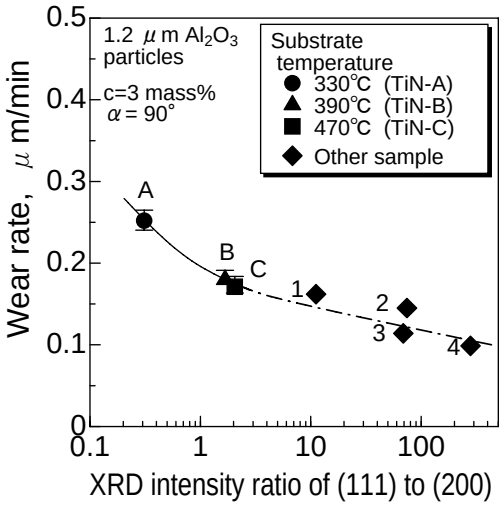

Detail of other samples

No.	Deposition technique	Coating thickness, μm	Nano-indentation hardness(49mN), GPa
1	MS	2.4	45.8
2	REB	2.8	53.6
3	MS	3.9	44.0
4	HCD	2.0	40.4

MS: Magnetron sputtering
REB: Reactive electron beam evaporation
HCD: Hollow cathode dischage

Fig.12 Relationship between XRD intensity ratio of (111) to (200) and wear rate.

It is well known that TiN coating consists of a NaCl type phase with FCC structure. For this structure, cleavage fracture tends to occurs on the {100} plane and the surface energy (γ) on each plane is approximately calculated as follows [16].

$$\gamma_{\{100\}} : \gamma_{\{110\}} : \gamma_{\{111\}} = 1 : \sqrt{2} : \sqrt{3}$$

Cleavage fracture on {100} plane occurs easier than the {111} in inverse proportion to the surface energy. Here, when comparing the wear rates between the TiN

coatings which show the largest and the smallest ratio of (111) to (200) in Fig. 12, the ratio of the wear rate (No. 4 to No. A, see Fig.12) is 0.37, which is similar value to the reciprocal of the ratio of surface energy of {111} to {100}, i.e. 0.58. From this discussion, the wear is likely to occur by tiny cleavage fractures in each grain.

Generally, it is shown that the slurry jet erosion technique can assess the quality of TiN coatings in terms of wear resistance, ductility and fracture resistance. The detailed mechanisms of material removal during this slurry jet erosion are not fully revealed. However, the damage scale is not even resolvable in AFM. It is possible that the damage scale is so small that the TiN wear is dominated by removal of the oxide scale, but a combination of such an oxidative wear with mechanical particle erosion of TiN is the most probable. Further analytical studies are needed to clarify this.

4 CONCLUSIONS

1. The slurry jet test is fast, easy to accomplish, and generates reproducible results. It is also very sensitive to variations in coating quality.
2. Since it produces very tiny wear craters, it is close to being non-destructive, and can easily be used on e.g. metal cutting inserts without affecting their performance.
3. For the coatings included in this study, the TiN deposited under the highest substrate temperature proved to have the highest wear resistance although it had a relatively low hardness, probably because of a corresponding improvement in ductility.
4. Another observation was that the wear rate varies with the TiN grain orientation, i.e. the {111} orientation shows higher wear resistance than the {100}, which correlates to a correspondingly higher cleavage fracture resistance within each grains.
5. Our proposed slurry jet erosion proved to be very useful and sensitive as a screening test when evaluating the properties of coatings including morphology and wear resistance.

ACKNOWLEDGEMENTS

The authors are grateful to Mr. N. Kasugai, student of University of Fukui, for his help in experiment, and Prof. H. Uchida and Prof. M. Yamashita, University of Hyogo, for their useful discussion

REFERENCES

[1] K.Holmberg, A.Matthews, Coating Tribology, Tribology Series 28, Elsevier, Amsterdam (1994).

[2] S.Hogmark, S.Jacobson, M.Larssson, U.Wiklund, Mechanical and tribological requirements and evaluation of coating composites, Modern Tribology Handbook II, B.Bhushan Eds., CRC Press (2001) 931-963.

[3] D.M. Kennedy, M.S.J. Hashmi, Methods of wear testing for advanced surface coatings and bulk materials, Journal of Materials Processing Technology, 77 (1998) 246-253.

[4] J.C.A. Batista, C. Godoy, G. Pintaude, A. Sinatora, A. Matthews, An approach to elucidate the different response of PVD coatings in different tribological tests, Surface and Coating Technology, 174-175 (2003) 891-898.

[5] I.M.Hutchings, Abrasive and erosive wear tests for thin coatings: a unified approach, Tribology International, 31, 1-3 (1998) 5-15.

[6] M.Bromark, M.Larsson, P.Hedenqvist, M.Olsson, S.Hogmark, E.Bergman, PVD coatings for tool applications: Tribological evaluation, Surface Engineering, 10, 3 (1994) 205-214.

[7] M.Bromark, M.Larsson, P.Hedenqvist, S.Hogmark, Determination of coating erosion resistance using the mass-loss technique, Proc. of the 6th Nordic Symposium on Tribology, Nordtrib '94 (1994) 207-213.

[8] R.J.K.Wood, Y.Puget, K.R.Trethewey, K.Stokes, The performance of marine coatings and pipe materials under fluid-borne sand erosion, Wear, 219 (1998) 46-59.

[9] Y.Iwai, K.Numbu, Slurry wear properties of pump lining materials, Wear, 210 (1997) 211-219.

[10] Y.Iwai, T.Honda, Y.Yamada, T.Matsubara, M.Larsson, S.Hogmark, Evaluation of wear resistance of thin hard coatings by a new solid particle impact test, Wear, 251 (2001) 861-867.

[11] Y.Iwai, Y.Ueno, T.Suehiro, T.Honda, S.Hogmark, Evaluation of wear resistance of PVD coatings on drills by using a slurry jet impact test, Proceedings of ASIATRIB 2002 International Conference, Jeju Island, Korea (2002) 141-142.

[12] I.M.Hutchings, Tribology: Friction and Wear of Engineering Materials, Edward Arnold, London, (1992) 133-197.

[13] L.A. Dobrzanski, M. Adamiak, G.E. D'Errico, Relationship between erosion resistance and the phase and chemical composition of PVD coatings deposited onto high-speed steel, Journal of Materials Processing Technology, 92-93 (1999) 184-189.

[14] S. Soderberg, S. Hogmark, U. Engman, H. Swahn, Erosion classification of materials using a centrifugal erosion tester, Tribology International, Dec. 1981, 333-344.

[15] K.J.Stout, L.Blunt, Three Dimensional Surface Topography, Penton Press (2000) 157.

[16] K.Endo, Surface Engineering, Yokendo (1987) 12 (in Japanese).